ELSEVIER

An efficient numerical calculation of wave loads on an array of vertical cylinders

Songping Zhu and Grant Moule

Department of Mathematics, The University of Wollongong, Wollongong, New South Wales, Australia

As is well known, most off-shore oil platforms are supported by vertical cylinders. Correctly and efficiently calculating the wave loads on an array of cylinders is of great concern to ocean engineers. It was shown by Au and Brebbia[1] that wave loads on vertical cylinders can be calculated by using the boundary element method (BEM). However, their boundary discretization turns out to be still quite costly when the wave loads on an array of a large number of cylinders need to be calculated. In this paper, a simple yet effective improvement on the numerical calculation of wave loads on vertical cylinders using BEM is presented. We shall show a new algorithm of boundary discretization designed to enhance the numerical efficiency and thereby to reduce the computational cost when an array of a large number of cylinders are involved in a calculation.

1. Introduction

With the construction of large off-shore structures, such as oil platforms which consist of a number of legs, the calculation of wave-induced forces on an array of cylinders has become increasingly important in recent years since the design of and the operation on such large structures rely very much on the reliability of predicting the wave-induced responses of the structures. For example, in order to avoid excessive structural vibrations, which are usually very difficult to eliminate completely, reasonably good vibrational analysis needs to be carried out during the design phase. The closeness of such vibrational analyses to reality is crucially dependent on a correct prediction of the wave-induced forces on each of the legs of an off-shore structure. Much research works in this area has been carried out in the past.

For the forces on a single vertical circular cylinder resting on the ocean floor and piercing the water surface, an analytical solution was found by MacCamy and Fuchs[2] in 1954. For a cylinder of arbitrary cross-section, only numerical solutions are available so far. The hybrid element method used by many researchers in this area[3,4] is a very powerful and robust method of calculating wave loads on a vertical cylinder of arbitrary cross-section. However, adopting this method can be computationally quite expensive especially for those incident waves with short wave lengths, since a large number of elements are needed in order to resolve waves within a wavelength[7]. Au and Brebbia[1] showed that the BEM is a numerically efficient alternative to solving the problem.

Wave diffraction around an array of cylinders is much more complicated than that around a single cylinder. Forces on each individual cylinder may vary considerably; some of them may experience larger forces and some may experience smaller forces compared with the forces they would have experienced if they were standing alone in an ocean with the same incident waves. Analytical solutions are rare for this case and they are very restrictive as far as the cylinder cross-sectional shapes are concerned. For an array of circular cylinders, Mingde and Yu[8] used the multiple scattering techniques developed by Spring and Monkmeyer[9] to study the case of shallow water wave diffraction of multiple circular cylinders. Chakrabarti[10] extended Spring and Monkmeyer's analysis to the complex field, which doubled the numerical efficiency in the final calculation for the solution. Spring and Monkmeyer's multiple scattering technique was further improved by Linton and Evans[11] in 1990. However, their solutions are only applicable to the case that the solution for a single cylinder exists, such as the case that only circular cylinders are involved.

With the advantage of being relatively simple to formulate the problem and computationally efficient to carry out the final calculation for the solution, approximation methods were proposed to calculate wave forces on an array of cylinders. Massel[12] presented an approximate solution of an infinite row of equally spaced cylinders at an arbitrary angle to the incident waves. However, his approximation theory is valid only for small ka values, where k is the incident wave number and a is the radius of the equal cylinders. Based on Simon's idea[13], McIver and Evans[14]

Address reprint requests to Dr. Songping Zhu at the Department of Mathematics, The University of Wollongong, P.O. Box 1144, Wollongong, NSW 2500, Australia.

Received 29 November 1993; revised 8 August 1994; accepted 19 September 1994

Appl. Math. Modelling 1996, Vol. 20, January

655 Avenue of the Americas, New York, NY 10010

0307-904X/96/$15.00
SSDI 0307-904X(95)00108-V

later proposed another approximation method, in which scattered waves from one cylinder are replaced by a plane wave of appropriate amplitude in the neighborhood of another cylinder. Their results compared favorably with those of Spring and Monkmeyer[9]. Although some good results were also presented using their approximation theory when the spacing between cylinders is small, McIver and Evan's theory was essentially based on the assumption of large spacing between cylinders and therefore limited the range of its application.

Numerical solutions to the diffraction of water waves around an array of cylinders seem to be inevitable and many works have been published in the past. The hybrid element method[7] is still usable. However, the high computational cost associated with the method, especially when the incident wavelength is short, motivated the search for more efficient methods. Using a vertical line wave source Green's function, Isaacson[15] calculated wave loads on an array of cylinders. The constant sources he placed are equivalent to the constant elements in the standard BEM later used by Au and Brebbia[1] who showed that most accurate results were produced by adopting quadratic elements and that constant elements were indeed superior to linear elements in calculating wave-induced forces on a single cylinder. However, the computational cost associated with adopting quadratic elements is too high when the number of cylinders is large; constant elements are preferable.

In this paper we shall show a simple yet very effective new discretization of cylinder boundaries with constant boundary elements. With this new discretization, fewer elements are needed to achieve the same numerical accuracy. A significant saving in CPU time has been achieved when the number of cylinders involved in a calculation is large.

2. Governing differential system

Consider the case that plane incident waves with the wave potential

$$\Phi^{(I)} = \frac{-iga_0}{\omega}\frac{\cosh\{\kappa(z+h)\}}{\cosh(\kappa h)} \times \exp\{i(\kappa_x x + \kappa_y y - \omega t)\} \quad (1)$$

are diffracted by an array of vertical cylinders resting on the ocean floor and piercing the water surface as shown in

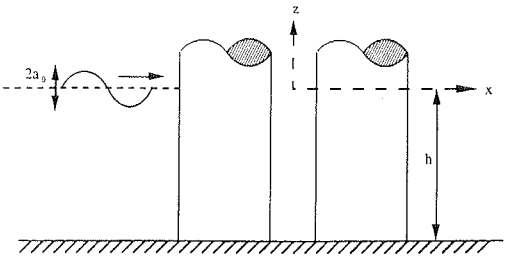

Figure 1. Waves incident on vertical cylinders.

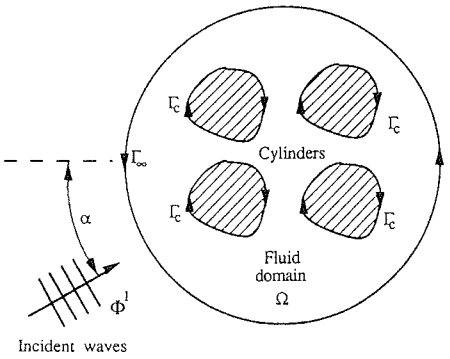

Figure 2. Boundaries around the fluid domain.

Figure 1. In equation (1), $i=\sqrt{-1}$, a_0 is the wave amplitude, h is the water depth, ω is the angular frequency, g is the gravitational acceleration, and κ_x, κ_y, are wave numbers in the x, y directions, respectively.

The governing equations and the boundary conditions for the scattered wave field, with the assumption that sea water is inviscid and incompressible and flow is irrotational, are

$$\nabla^2\phi + \kappa^2\phi = 0 \quad (2)$$

subject to the following boundary conditions

$$\frac{\partial\phi}{\partial n} = -\frac{\partial\phi^{(I)}}{\partial n} \quad \text{on } \Gamma_c \quad (3)$$

$$\frac{\partial\phi}{\partial n} - i\kappa\phi = 0 \quad \text{on } \Gamma_\infty \quad (4)$$

where κ is the total wave number defined as

$$\kappa = \sqrt{\kappa_x^2 + \kappa_y^2} \quad (5)$$

and Γ_c indicates the boundaries formed by the surfaces of the cylinders, Γ_∞ stands for a fictitious boundary at infinity for the time being, as shown in *Figure 2*, and n is the coordinate in the direction of the unit outward vector $\mathbf{n}$ normal to Γ_c and Γ_∞. Boundary condition (3) states that waves are totally reflected on the surface of the cylinders. Boundary condition (4) is the Sommerfeld radiation conditions,[16] which simply states that the energy associated with the scattered waves will propagate toward infinity without being reflected back. Notice that the scattered waves are of the same angular frequency ω, which is related to the wavelength, κ, from the dispersion relation

$$\omega^2 = g\kappa \tanh(\kappa h) \quad (6)$$

Following Au and Brebbia,[1] a boundary integral equation can be formulated based on the Galerkin method. Since this integral equation as well as its discretized matrix form with N boundary elements being placed on the boundary Γ_c are now very much standard in the BEM literature, they are not presented here. Once the discretized integral equation is solved for the N nodal values of the unknown function ϕ, other physical properties such as water run-up, the total wave induced force, and moment can be readily calculated. However, when the number of

cylinders involved in the calculation is large, it would be of a great advantage computationally if the number of elements could be kept as low as possible while a certain numerical accuracy level is maintained. It was through a new discretization as outlined in the following section that our improvement on the calculation emerged.

3. Boundary discretization

The boundary element method requires the boundary of the cross-section of the cylinder to be discretized into a finite number of elements. Au and Brebbia[1] showed that for wave diffraction problems, linear elements resulted in the worst numerical accuracy. However, although quadratic elements can yield more accurate results than constant elements do, they are generally more expensive in terms of computational time. When the number of cylinders involved in the calculation is large, one really likes to use as few constant elements as possible and to preserve a certain numerical accuracy in the mean time.

For constant elements, each element is deemed to be a straight line with the node placed at the center of the element. The shape formed by all these constant boundary elements is a polygon which approximates the cylinder's cross-section. The traditional way of positioning these elements is to place the end points of each element on the boundary of the cross-sectional shape. As the number of elements increases, the polygon so formed better approximates the cylinder cross-section. This is shown in *Figure 3*.

For a convex cylinder cross-section, such as a circle, the polygon lies entirely inside the cylinder cross-section. The perimeter of this polygon associated with the above discretization is smaller than the perimeter of the circle. When the wave-induced forces are calculated, the pressure on the surface of a cylinder is summed up vectorially after being multiplied by an infinitesimal area and integrated over the entire boundary surface. Therefore, the total wave force is directly related to the surface area of the cylinder exposed to the waves. For a cylinder of uniform cross-section, the perimeter of the cross-section determines the total

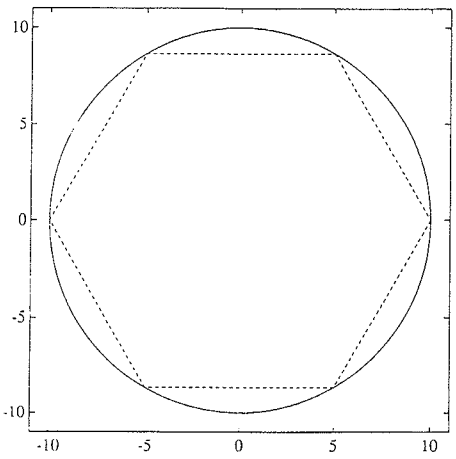

Figure 3. Traditional discretization.

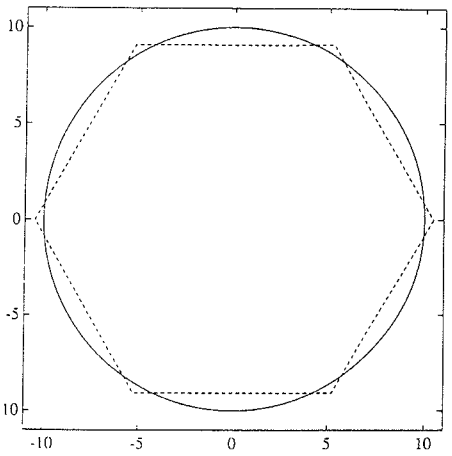

Figure 4. New discretization.

area of the cylinder exposed to the waves. Thus, better results should be obtained with the BEM if the polygon formed by the boundary elements has the same perimeter as that of the original cylinder cross-section.

For a circular cylinder of radius r a regular polygon of n sides has the same perimeter if it is inscribed in a circle of radius R, where

$$R = \frac{r\pi}{n \sin\frac{\pi}{n}} \tag{7}$$

Such a polygon is shown in *Figure 4*.

This idea can be extended to shapes other than circles. For a cylinder of arbitrary cross-section, an algorithm is needed in order for a computer to generate automatically a polygon that is of the same perimeter as that of the original cylinder. The radius r in equation (7) now needs to be replaced by the local radius of curvature, which determines the distance that an end point is moved along the straight line passing through the original intersection point of two elements and in the direction $\mathbf{N}_i$, which is obtained by simply averaging the normals of the two adjacent elements as shown in *Figure 5*. A flow chart of the algorithm is included in the Appendix.

The adoption of such an algorithm in the discretization of the boundary generates a polygon that is of the same perimeter as the original boundary contour. The computational time required for this new discretization process is

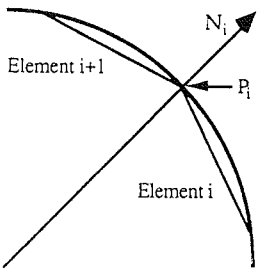

Figure 5. An illustration of the straight line along which the end point P_i is moved.

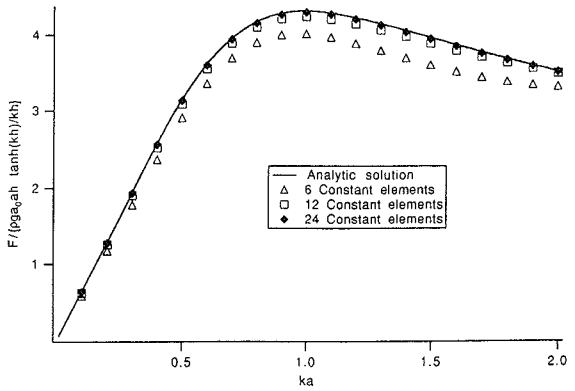

Figure 6. Wave-induced forces on a single circular cylinder with traditional discretization.

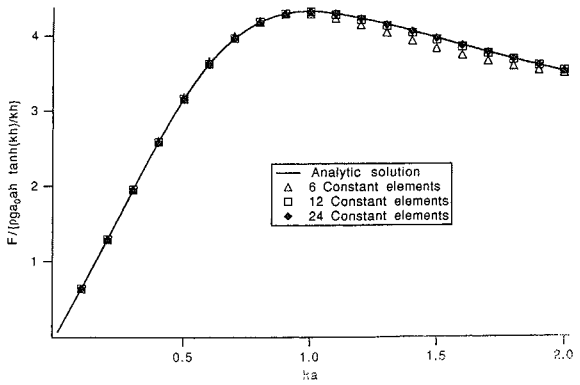

Figure 7. Wave-induced forces on a single circular cylinder with new discretization.

much less than the additional computational time required in the traditional discretization with the extra number of elements needed to achieve the same numerical accuracy. In order to test the new algorithm, several numerical tests were carried out and all the results showed the high efficiency and reliability of the algorithm in generating a polygon that is of the same contour length as the original contour. As a very special case, discretizing a circle only requires one iteration. With a couple of iterations, the discretization of the boundary of an ellipse can be finished. If a sufficient number of elements are used initially, few iterations are needed for even more complex nonconvex boundary shapes.

In order to show the numerical efficiency achieved by adopting the new discretization, wave forces exerted on a circular cylinder are calculated and compared with the analytical solution given by MacCamy and Fuchs.[2] In all of the following numerical examples, the radius of the cylinder, a, was taken to be 10 m and the water depth, h, was taken to be 50 m.

Figure 6 shows the convergence of the numerical solution to the analytical solution as the number of boundary elements increases using the traditional discretization; the nondimensional total horizontal force, $F/\{\rho g a_0 h \tanh(kh)/kh\}$, is plotted against κa. The convergence of the numerical scheme when the number of elements increases is evident. As can be clearly seen from *Figure 6*, the numerical error is rather large for $\kappa a > 1.0$, if one tries to use a small number of elements such as 6. The numerical accuracy was significantly improved when the new discretization was adopted. Similar results as those shown in *Figure 6* are now shown in *Figure 7* with the new discretization being used. It is amazing to see that a simple idea such as demanding that the perimeter of the boundary elements in a discretization be equal to that of the original cross-section can lead to a greatly enhanced numerical accuracy. By using as few as six constant boundary elements the new discretization produces values for the total horizontal force that are in very good agreement with the analytical result.

In order to get some quantitative idea of the improvement that the new discretization can generate, the relative errors in the total horizontal force of the two discretization methods for the case of $\kappa a = 1$ are tabulated in *Table 1*. As can be seen from *Table 1*, the new discretization is approximately ten times more accurate than the results obtained using the traditional discretization with the same number of boundary elements being used.

Higher order boundary elements can be used to produce more accurate results[1,17]. However, the adoption of these higher order elements such as quadratic elements requires more nodes per element and thereby results in larger matrices to be solved. Furthermore, more numerical integrations on each node need to be carried out for higher order elements. Hence the computational time required by using higher order elements will also be increased, especially when a large number of elements are required in the case that the number of cylinders involved in a calculation is large. In addition, some of the higher order elements may not necessarily produce better results. Linear elements were shown, for instance, to produce worse results than constant elements.[1] Nevertheless, one still needs to compare the numerical accuracy achieved by adopting higher order elements such as quadratic elements with that achieved by adopting constant elements with new discretization. In *Figure 8*, the relative numerical errors resulting from using constant boundary elements with the traditional and the new discretizations and quadratic elements are plotted against the total CPU time required for different numbers of elements. As the number of elements increases, for all three cases, the numerical accuracy im-

Table 1. Computed forces and relative errors versus the number of elements used

Elements	Traditional discretization		New discretization	
	Force	% Error	Force	% Error
6	4.009	7	4.276	0.8
8	4.141	4	4.294	0.3
12	4.234	2	4.302	0.2
24	4.290	0.4	4.307	0.04

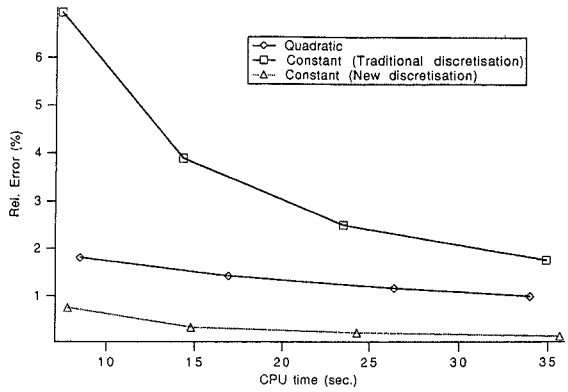

Figure 8. Relative errors vs. CPU time for different elements.

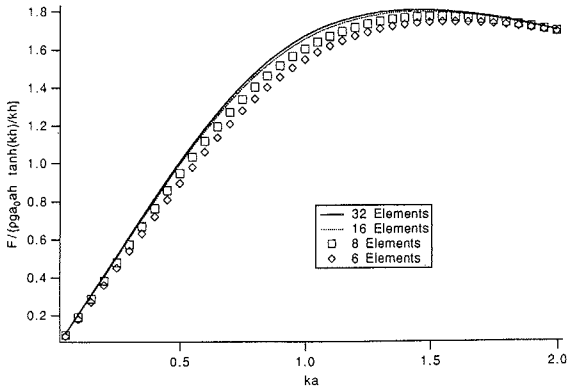

Figure 10. Plane waves incident on an elliptical cylinder using the traditional discretization.

proved while the total CPU time increases, which is expected. However, not only is the new discretization far superior to the traditional discretization, but also the results obtained by adopting the new discretization is surprisingly much better than those obtained by adopting quadratic elements.

The next question one may naturally raise is whether or not choosing equal perimeter for the discretized polygon yields the optimum results in terms of numerical accuracy. *Figure 9* shows the variation of the relative error with the ratio of the perimeter of the discretized polygon to that of the original circle. The relative error for each perimeter is calculated as the average relative error for five different wave numbers, varying up to κa equal to 1. The relative error at the vertical axis represents the error of the traditional discretization. From this graph it can be seen that the point where the perimeters are equal (indicated by a little solid square) is very close to the point of minimum error. Therefore by making the perimeter of the polygon formed by the constant elements equal to that of the cross-sectional boundary of the cylinder, the relative error is reduced to a value very close to its minimum value for a particular number of elements. In doing so, the error is reduced by a factor of ten, which has also been demonstrated in *Table 1*. This is quite significant since the CPU time is roughly proportional to the square of the number of elements used; for a desired accuracy the new discretization can lead to the same results in significantly less time.

Some quantitative measurement on the numerical efficiency can also be obtained from analyzing data present in *Figure 9* and *Table 1*. For a given accuracy it takes about one third the number of elements using the new discretization and approximately one ninth of the computational time is saved.

To further test the robustness of the new algorithm used in the discretization of the boundary of a noncircular cylinder, wave force exerted on an elliptical cylinder with the minor axis half the length of the major axis ($a = 10$ m) is now calculated and compared with the analytical solutions given by Goda and Yoshimura.[5] The discretization was again completed after one iteration. The total forces are calculated with different numbers of elements and the results are shown in *Figure 10* with the traditional discretization being utilised and in *Figure 11* with the new discretisation being utilized. Clearly, the new discretization converges faster than the traditional method in a similar fashion to the case of a circular cylinder shown in *Figures 6* and *7*.

The relative errors using 16 elements of both the traditional and new discretization for the wave-induced forces on an elliptical cylinder are shown in *Figure 12*. It can be seen that the new discretization again produces fewer numerical errors than the traditional discretization does. *Figure 13* shows the numerical results for wave-induced forces on an elliptical cylinder by using 8 elements with

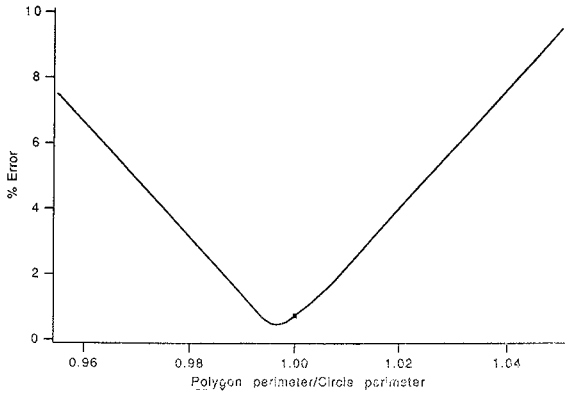

Figure 9. The variation of relative errors with polygon perimeter.

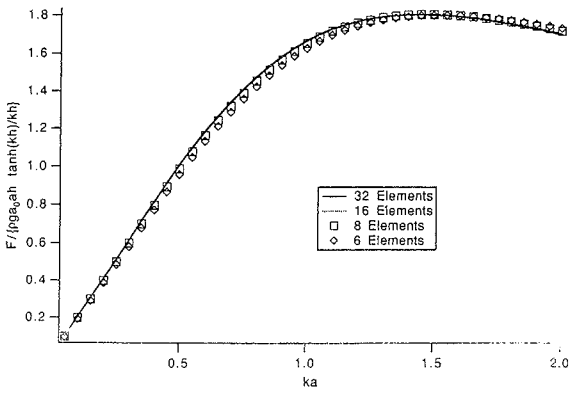

Figure 11. Plane waves incident on an elliptical cylinder using the new discretization.

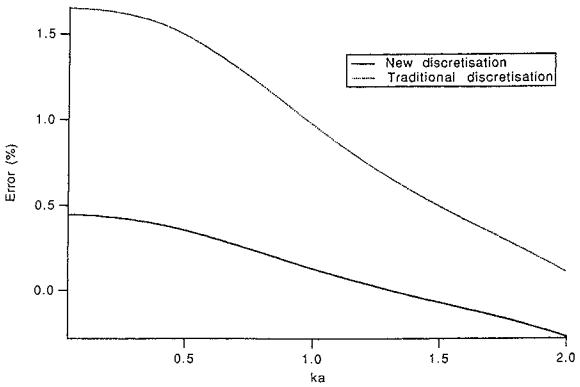

Figure 12. Relative errors with 16 constant elements used for plane waves incident on an elliptical cylinder.

the new discretization versus using 16 elements with the traditional discretization. Doubling the number of elements with the traditional discretization produces results that are of nearly the same accuracy as the new discretization, but this takes about four times the CPU time to compute. Hence the results of the same accuracy level can be obtained by using the new discretization while only requiring a quarter of the CPU time used by the traditional method.

4. Computational results and discussion

With the new discretization, we were able to reduce the computational time involved in computing the force on an array of cylinders substantially. As a numerical example, we computed the wave-induced forces on an array of four cylinders arranged as shown in *Figure 14*.

Unlike a singular cylinder being placed in water, the wave-induced forces on each individual cylinder in an array can vary vastly, depending on how the cylinders are placed as a whole, how large each cylinder is, how far they are separated, and of course at which direction and of what wavelength the incident waves are relative to the array. To measure the closeness of the cylinders, the smallest distance between the edges of any pair of cylinders is defined as the cylinder separation.

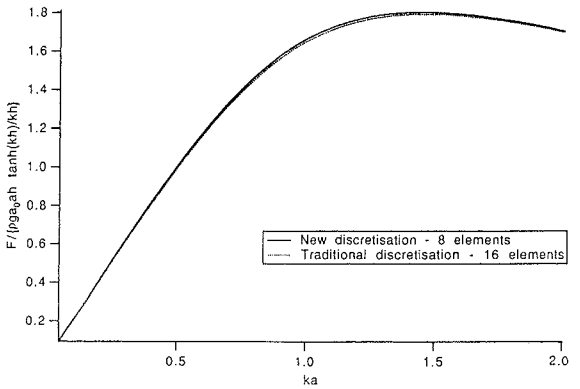

Figure 13. Wave-induced forces on an elliptical cylinder.

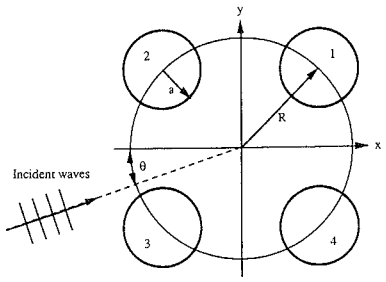

Figure 14. Waves incident on an array of four cylinders.

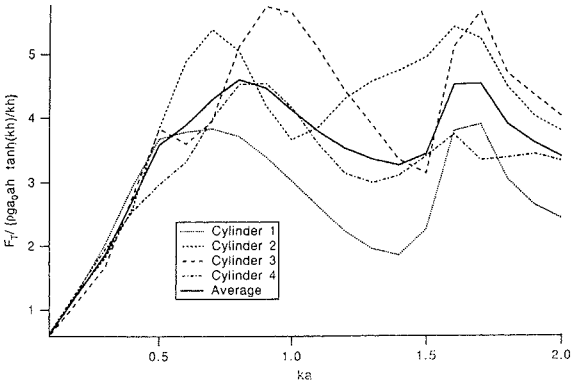

Figure 15. Wave forces on an array of four cylinders with an incident angle of 30° and a cylinder separation of $2a$.

Figure 15 shows the wave-induced forces on each of the four circular cylinders being placed with cylinder separation equal to $2a$, where a is the radius of each cylinder and is given a value 10 m for all the following numerical examples. The angle of incident, α, was taken to be 30° and the water depth was again taken to be 50 m. From this figure, one can clearly see that the wave forces on each cylinder vary as κa increases. Some cylinders in an array may experience larger forces compared with those they would have experienced if they were standing alone in the sea water. For example, when $\kappa a = 1.0$, the nondimensional force on cylinder 3 is about 5.7, which is about 40% more than the nondimensional force on a single cylinder with the same κa.

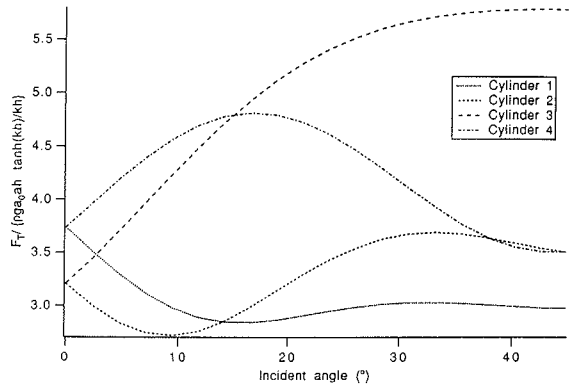

Figure 16. Wave forces on an array of four cylinders with a ka of 1.0 and a cylinder separation of $2a$.

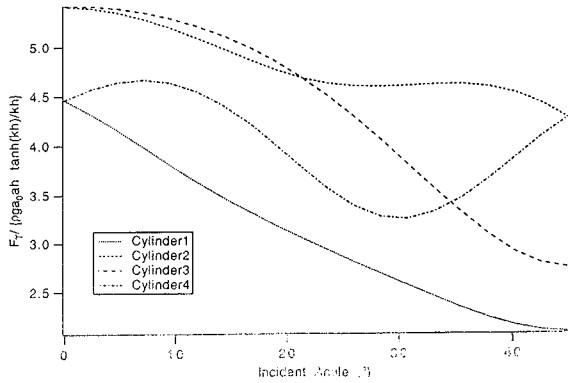

Figure 17. Wave forces on an array of four cylinders with a *ka* of 1.0 and a cylinder separation of 3*a*.

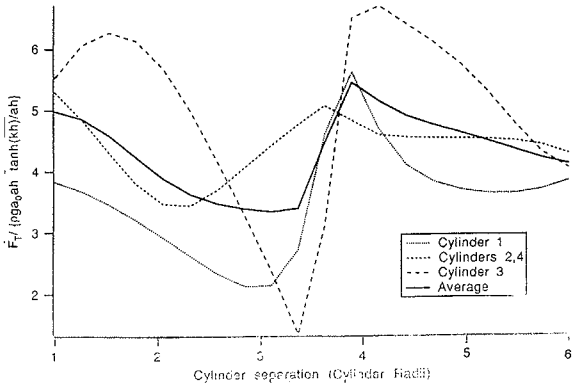

Figure 19. Wave forces on an array of four cylinders with a *ka* of 1.0 and an incident angle of 45°.

The wave-induced forces on each individual cylinder vary with the angle of incidence as well. In *Figure 16*, the variation of the nondimensional forces are plotted against the incident angle of the incident waves when κa and the cylinder separation are fixed with 1.0 and $2a$, respectively. At zero incident angle, cylinders 1 and 4 experience the same wave-induced forces and so do cylinders 1 and 3 due to the symmetry of the cylinders with respect to the incident waves. As expected, when the incident angle becomes 45°, cylinder 3 experiences the largest force because all the other cylinders are in the "shadow" of cylinder 3. This again shows that care must be taken when designing an array of cylinders to withstand the wave-induced forces; at certain incident angles, one cylinder could have taken all the wave loads whereas others are not doing their jobs.

It is very interesting to have observed that the front cylinder (e.g., cylinder 3 when the incident angle is 45°) does not always necessarily experience the largest force. In *Figure 17*, again the nondimensional forces versus the incident angle are plotted in the same way as in *Figure 16* except the cylinder separation now is $3a$. When the incident angle is equal to 45°, the forces on cylinders 2 and 4 are larger than that on the front cylinder 3, which is "unexpected" in the common sense. This shows that the diffraction around an array of cylinders are really complicated and the forces on each individual cylinder may depend on a number of factors such as the cylinder separation here. To have a clear view of the wave-induced forces varying with the cylinder separation, the nondimensional forces versus the cylinder separation are plotted in *Figure 18* for the incident angle being zero and $\kappa a = 1.0$. The largest forces seem to be exerted on all cylinders when the cylinder separation is about 3.3 times the radius of each individual cylinder for an incident angle of zero. For an incident angle equal to 45°, quite opposite conclusions are drawn as shown in *Figure 19*, in which all the quantities are the same as in *Figure 18* except the incident angle now is 45°.

All these results indicate that the behavior of wave-induced forces associated with diffraction around an array of cylinders is very complicated and cannot readily be determined from the results of the diffraction around a single cylinder. As the number of cylinders in an array increases, the use of the new discretization method would significantly reduce the computational time required and allow the calculation of the wave forces on an array of a large number of cylinders to be numerically more efficient.

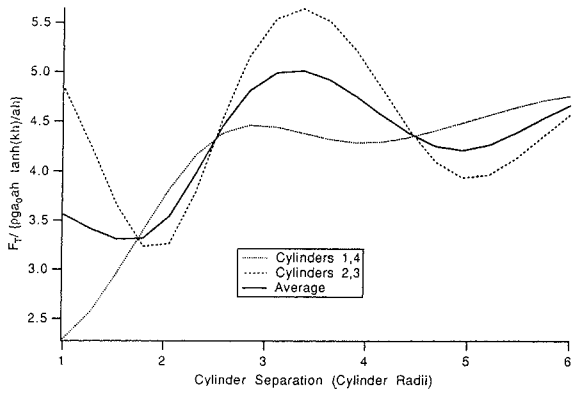

Figure 18. Wave forces on an array of four cylinders with a *ka* of 1.0 and an incident angle of 0°.

5. Conclusions

In this paper, a simple improvement on the numerical calculation of wave loads on vertical cylinders has been shown to be very effective. This improvement involves a new discretization for the constant boundary elements such that the perimeter of these elements is close to the perimeter of the cylinder cross-section. By using the new discretization, the accuracy of numerical results increases significantly, even when compared with quadratic boundary elements for the same computational time. When an array of cylinders is considered, the new discretisation provides a simple way of reducing the total number of constant boundary elements required, resulting in great savings in computational time, allowing larger arrays of cylinders to be examined efficiently.

Wave diffraction around an array of cylinders is quite complicated, especially with cylinders of arbitrary cross-sections. The wave-induced forces on each individual cylinder in an array can be quite different from those of a

single cylinder. For a given separation and a particular type of cylinder cross-section, the incident angles and different wave lengths of incident waves must be examined when designing an off-shore structure. Furthermore, short-crested waves may even exert larger wave forces on an array of cylinders since they have been found to exert larger wave forces on a single cylinder of noncircular cross-section[6]; their role will be discussed in a forthcoming paper.

Appendix

A flow chart of the new algorithm is shown below:

(1) Place n element end points on the perimeter of the shape (traditional discretization);
(2) For each element calculate its normal direction;
(3) At each element end-point i,
  (a) Calculate the angle, θ_i, between the normals of the two adjacent elements;
  (b) Find the direction, $\mathbf{N}_i$, which is obtained by simply averaging the normals of the two adjacent elements. (this will be the direction in which to move the end point);
  (c) Calculate the relative distance R_i by which the end point is moved. This relative distance is indirectly related to the local radius of curvature as:

$$R_i = \frac{1}{\sin\dfrac{\theta_i}{2}}\left(\frac{\theta_i}{2\sin\dfrac{\theta_i}{2}} - 1\right)$$

(4) Sum all the relative distances

$$S = \sum_{i=1}^{n} 2R_i \sin\frac{\theta_i}{2},$$

(5) Calculate the difference in perimeters D = original shape perimeter-polygon perimeter;
(6) Move each of the element end points in the calculated direction, $\mathbf{N}_i$, with the distance DR_i/S;
(7) Repeat steps (5) and (6) until D is sufficiently small or the polygon perimeter is close enough to the shape perimeter.

References

1. Au, M. C. and Brebbia, C. A. Diffraction of water waves for vertical cylinders using boundary elements. *Appl. Math. Modelling* 1983, **7**, 106–114
2. MacCamy, R. C. and Fuchs, R. A. Wave forces on piles: a diffraction theory. *US Army Corps of Engineering, Beach Erosion Board, Technical Memorandum* No. **69**, 1954
3. Chen, H. S. and Mei, C. C. Oscillations and wave forces in a man-made harbor in the open sea. *Proceedings of the 10th Symposium on Naval Hydrodynamics*. Cambridge, MA, 1974, pp. 573–596
4. Houston, J. R. Combined refraction and diffraction of short waves using the finite element method. *Appl. Ocean Res.* 1981, **3**, 163–170
5. Goda, Y. and Yoshimura, T. Wave force on a vessel tired at off-shore dolphins. Chapter 96, *Proceedings of the 13th Coastal Engineering Conference*, Vol III. 1972, pp. 1723–1742
6. Zhu, S.-P. and Moule, G. Numerical solution of short-crested waves around a vertical cylinder of arbitrary cross-section. *Ocean Eng.* 1994, **21**(7), 645–662
7. Mei, C. C. Numerical methods in water-wave diffraction and radiation. *Ann. Rev. Fluid Mech.* 1978, **10**, 393–416
8. Mingde, S. and Yu,P. Shallow water diffraction around multiple large cylinders. *Appl. Ocean Res.* 1987, **9**, 31–36
9. Spring, B. H. and Monkmeyer, P. L. Interaction of plane waves with vertical cylinders. Chapter 107. *Proceedings of the 14th International Coastal Engineering Conference*, 1974, pp. 1828–1845
10. Chakrabarti, S. K. Wave forces on multiple vertical cylinders. *J. Waterway Port Coastal Ocean Div. ASCE*, 1978, **104**, 147–161
11. Lindon, C. M. and Evans, D. E. Interaction of waves with arrays of vertical circular cylinders. *J. Fluid Mech.* 1990, **215**, 549–569
12. Massel, S. R. Interaction of water waves with cylinders barrier. *J. Waterway Port Coastal Ocean Div. ASCE*, 1976, **102**, 165–187
13. Simon, M. J. Multiple scattering in arrays of wave-energy devices. *J. Fluid Mech.* 1982, **120**, 1–25
14. McIver, P. and Evans, D. V. Approximation of wave forces on cylinder arrays. *Appl. Ocean Res.* 1984, **6**, 101–107
15. Isaacson, M. and de St., Q. Vertical cylinders of arbitrary section in waves. *J. Waterway Port Coastal Ocean Div. ASCE*, 1978, **104**, 309–324
16. Sommerfeld, D. *Partial Differential Equations in Physics*. Academic Press, New York, 1949
17. Brebbia, C. A. Telles, J. C. F. and Wrobel, L. C. *Boundary Element Techniques: Theory and Applications in Engineering*. Springer-Verlag, 1984